

Geometric morphometric analysis of sexual dimorphism in the mandible from panoramic X-ray images

Emilio Nuzzolese¹
 Patrick Randolph-Quinney^{2,3}
 Jennifer Randolph-Quinney²
 Giancarlo Di Vella¹

¹Human Identification Laboratory,
 University of Turin (Italy)

²University of Central Lancashire,
 Preston (UK)

³University of Johannesburg,
 South Africa

Corresponding author:
emilio.nuzzolese@unito.it

The authors declare that they have
 no conflict of interest.

KEYWORDS

Geometric morphometrics;
 Sexual dimorphism;
 Sex assessment;
 Forensic odontology

J Forensic Odontostomatol

2019, May;(37): 2-35:44

ISSN :2219-6749

ABSTRACT

The human mandible is routinely utilised as part of the assessment of biological identity in forensic anthropological and odontological practice. The research introduces a novel geometric morphometric technique to investigate and quantify shape variation in the morphology of the mandibular corpus and ascending ramus and consequently highlights the potential for forensic purposes. Human mandibles from digital clinical orthopantomogram X-ray images, based on a sample of 50 male and 50 female adults from a modern Italian population, were examined. Three fixed landmarks were applied to the symphysis and condyle and 50 semi-landmarks re-sampled along the inferior corpus and the posterior ramus. Symmetrical reflection was applied yielding 200 configurations of 53 landmarks. Shape analyses were undertaken via: Procrustes superimposition; principal components analysis to investigate patterns of variation; classification using linear discriminant analysis with leave-one-out cross-validation; partial least squares (PLS) to test for structural modularity; and finally, retile page sampling and re-analysis following PLS to optimize shape classification criteria. Stepwise re-sampling of landmarks reached an optimum cross-validated classification of 94.0% based on 25 landmarks; the results are strongly significant and suggest that the shape relationship between the mandibular corpus and ramus offers significant potential for forensic identification purposes using this method.

INTRODUCTION

The human mandible is routinely utilised as part of the assessment of biological identity in forensic anthropological and odontological practice.¹ Various authors have pointed to the utility of odontological methods in morphological and metric features of teeth,² but also traditionally recovered morphological, metric, and non-metric traits in the mandible, including discrete areas such as symphyseal morphology and shape,³⁻⁶ gonial angle, gonial inversion and eversion,⁷⁻¹⁰ ramus flexure,^{11,12} overall shape from elliptical Fourier transforms¹³⁻¹⁵ and discriminant functions based on linear dimensions^{16,17} amongst others in the assessment of biological sex and ancestry.

More recently, a number of studies have utilised geometric morphometric (GM) approaches to address issues of biological identity in this anatomical region.¹⁸⁻²³ Defined simply, GM is the statistical analysis of form based on Cartesian landmark

coordinates.²⁴ GM techniques generally involve the capture of homologous landmarks which can be defined as precise locations on biological specimens that hold some functional, structural, developmental or evolutionary significance and are directly comparable between specimens. Landmarks can be recorded as two or three-dimensional co-ordinates which result in a spatial framework of the relative positions of the chosen points in two or three-dimensional space. Such data allows for the statistical analysis of the embedded shape geometry of a biological form through a variety of transformative or computational methods.²⁵⁻²⁹ The research presented here utilises geometric morphometric techniques to investigate and quantify shape variation in the morphology of the mandibular corpus and ascending ramus and consequently highlights the potential for forensic human identification. We present the results of a novel morphometric study using clinical panoramic scanning x-radiography, the aim of which was to develop a methodologically and statistically robust means of investigating biological variation in lower jaw morphology from a commonly acquired clinical data source which may be of use in the human identification process.

MATERIAL AND METHODS:

Digital orthopantomogram images (OPG) in TIFF format were acquired of the upper and lower

dentulous jaws of 50 Italian male and 50 female participants, derived from a larger clinical image database. The images were captured by odontologists using a panoramic digital device (Planmeca Proline xc) as part of private clinical dental practice, with permission obtained for the anonymised use of resulting OPG for research studies. The specimens utilised were drawn from a larger sample pool, with the age distribution of both sex cohorts matched using exact randomisation (male profile matched to female), resulting in a common demographic profile for both sexes (Fig. 1); this yielded a mean age of 38 years for males (minimum age 20 years, maximum age 68 years) and 37 years for females (minimum age 21 years, maximum age 62 years). The OPG images were stripped of biographical information, and re-labelled with a sequential numerical code which referenced sex and age only. Three type I and type III 2D landmarks were applied to the symphysis and condylar process using TPS Digit software and 50 re-sampled equidistant semi-landmarks were established along the inferior border of the corpus and the posterior border of the ascending ramus; semi-landmarks were anchored anteriorly and posteriorly to fixed homologous points (Table 1). Landmarks were reflected to the opposite side, providing n 200 configurations of k 53 landmarks (resulting in n 100 left and n 100 right side, k 53 each).

Fig. 1 Age profile of male and female cohorts used in this study. Mean ages: male 38 years, female 37 years. Range: male 20 to 68 years, female 21 to 62 years.

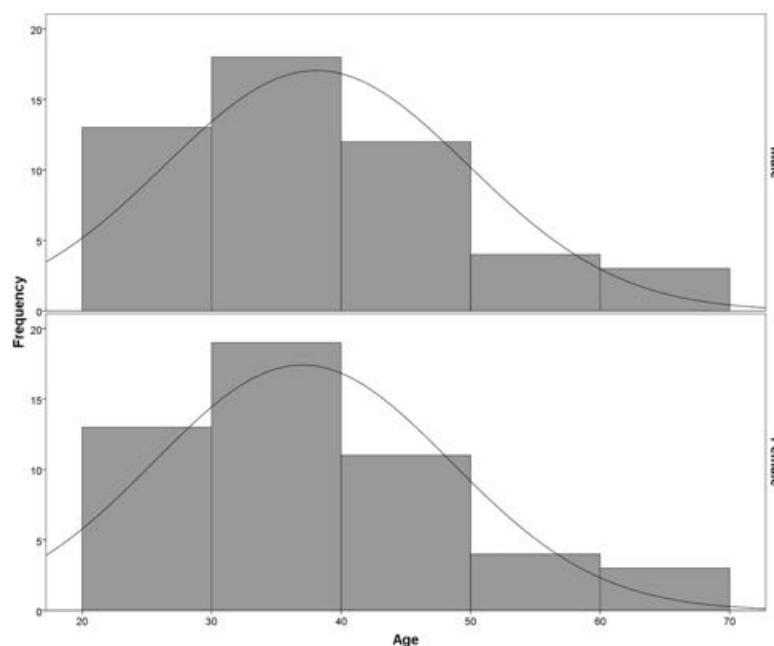


Table 1. Landmark definitions.

Landmark	Description
1	Infradentale
2	Most superior point on mandibular condyle
3	Most anterior point on mandibular condyle
4-33	Equidistant semi-landmark series captured along inferior border of mandibular corpus from gnathion to gonion
34-53	Equidistant semi-landmark series captured along posterior border of ascending ramus from gonion to the most postero-superior point on the mandibular condyle

The statistical shape analyses of the 2D coordinate configurations involved the following stages: (1) partial Procrustes superimposition (GPA) with full tangent space projection; (2) regression of tangent space distance onto Procrustes distance to test for tangent space approximation; (3) assessment of inter and intra-observer measurement error using a 5x5x5 repeat procedure, with Procrustes ANOVA to test for differences in group means; (4) principal components analysis (PCA) to reduce dimensionality and investigate patterns of population variation, with test for significance of shape differences between groups using Procrustes ANOVA; (5) classification using Fisher's linear discriminant analysis (LDA) with leave-one-out cross-validation to assess performance of the classification; (6) partial least squares (PLS) analysis within a single configuration to test for structural modularity; and (7) stepwise re-sampling and re-analysis of dataset following PLS to optimise shape classification criteria. Shape analyses were undertaken using the *shapes* library³⁰ and complementary *R* statistical routines,³¹ partial least squares analysis in *MorphoJ*³² and additional statistical analyses in *SPSS 20.0*.³³

RESULTS

The resulting two-dimensional coordinate configurations ($n = 200$) were subjected to a generalised Procrustes analysis (GPA) with full-tangent space projection and scaling invariance which effectively removes size from the analysis by scaling all configurations against unit centroid size³⁴ leaving only shape differences between configurations. Potential measurement error of

both intra and inter-observer landmark acquisition was assessed by two of the authors (PRQ and JRQ) digitising five individual configurations five times on five separate occasions and then subjecting the resulting configurations to GPA.

Procrustes ANOVA based on Procrustes distance³⁵ was used to assess the relative magnitude of error from repeat measurements; no significant differences were noted between test runs within and between each observer confirming that measurement error was low.

Further statistical analysis of shape requires that the Procrustes coordinate configurations are projected back into Euclidean tangent space,³⁴ with statistical analyses carried out within that space using standard multi-variate methods. The appropriateness of tangent space projection was tested by regressing the distance in tangent space onto Procrustes distance; this produced a correlation coefficient of 0.99 indicating that tangent projection and Procrustes approximation were successful. When dealing with such high dimensional data it is natural to reduce the dimension and a commonly used technique is principal components analysis (PCA), carried out by forming the sample covariance matrix of the residuals and computing the eigenvalues and eigenvectors accordingly. Following GPA, the mandibular configurations were subjected to PCA to explore the relationships within the global sample and specifically the patterns of sexual dimorphism between male and female forms. 102 principal components were

produced ($2k - 4 = 102$ shape variables), allowing for an investigation of overall shape variation in corpus and ramus morphology.

The first 10 principal components account for over 95% of shape variation in the sample (Table 2). Global shape variation is expressed in Fig. 2 by the plot of principal components 1 and 2 and shape variance by vector plots of the first three principal components in Fig. 3. As can be clearly seen, global variation is primarily manifested through the relative size differences in the height of the ascending ramus and placement of the inferior border of the symphysis (PC1), with higher order PCs displaying differential shape patterns in the orientation of the gonial angle compared to the symphysis and ascending ramus (PC2) and flexure of the inferior corpus and projection of the symphysis (PC3).

Table 2. Total population variance explained by principal components analysis (first 10 PC's only).

	Eigenvalue	% var	Cum %
PC 1	0.00099494	36.108	36.108
PC 2	0.00085379	30.985	67.093
PC 3	0.00030537	11.082	78.176
PC 4	0.00017213	6.247	84.423
PC 5	0.00011095	4.027	88.449
PC 6	0.00006511	2.363	90.812
PC 7	0.00006037	2.191	93.003
PC 8	0.00003876	1.407	94.410
PC 9	0.00002743	0.996	95.405
PC 10	0.00002138	0.776	96.181

Fig. 2 Visualization of global population shape variation showing results of principal components analysis based on covariance matrix of k 53 landmarks. Graph highlights first two principal axes of variation with markers indicating sex.

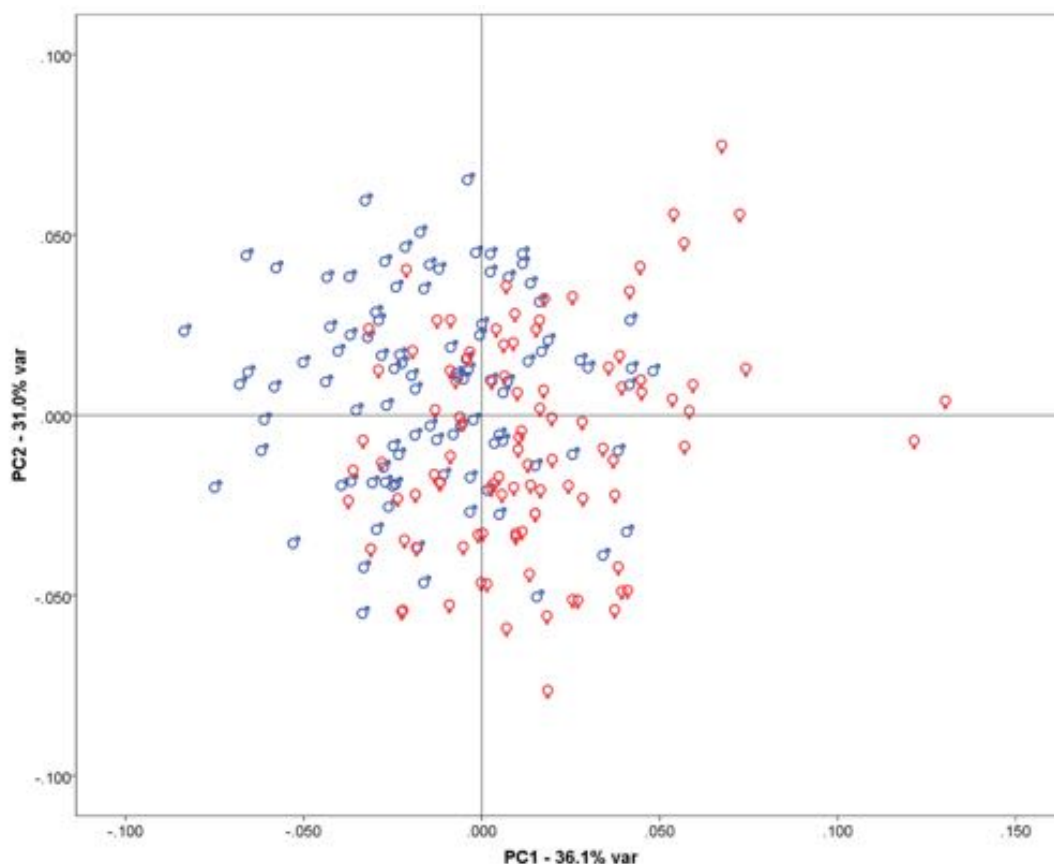
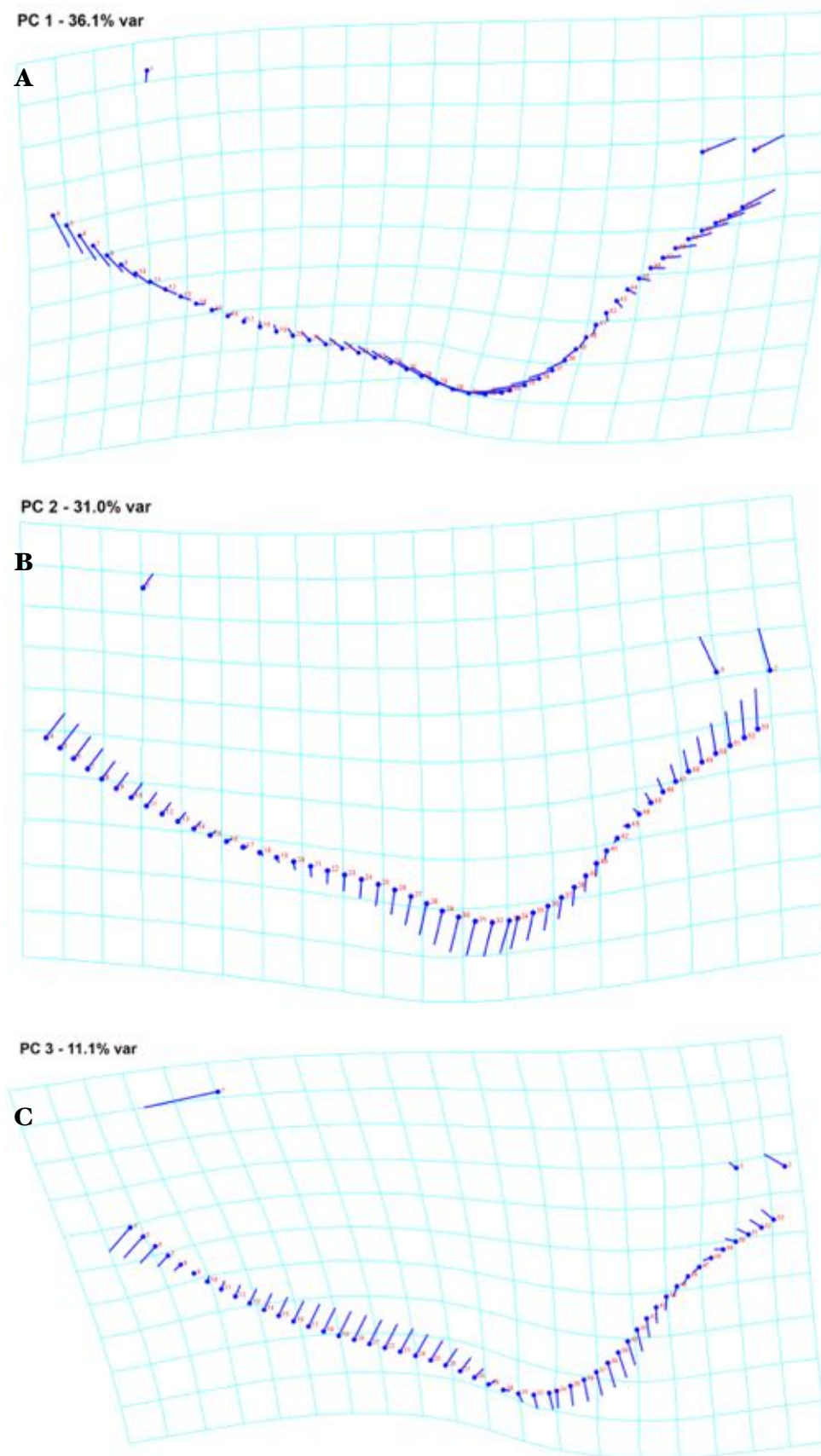


Fig. 3a to 3c Visualization of shape variation along the first, second and third principal component axes showing the extremes of shape variation as vectors compared to the consensus (mean) shape represented by solid circles, with deformation grid applied to assist visualization. Variation represented is PC1 36.11%, PC2 30.99% and PC3 11.10% respectively. Figures generated using *MorphoJ*.



The utility of the resulting shape variables as an aid in the assessment of biological sex was undertaken using Fisher's linear discriminant analysis based on the residual shape variables. Classification of specimens based on outlines or semi-landmarks often poses a challenge in GMM analyses in that accurate representation of a curve or surface requires many measurements, but this increase in the number of resulting shape variables dramatically increases the sample sizes necessary to carry out discrimination,³⁶ otherwise known as the curse of dimensionality.

One way to circumvent this is to convert the shape variables into principal component scores and reduce the dimensionality of the data by analysing a limited number of PC scores from the cases instead of the original data,³⁷ thus only relatively large group mean differences will be represented by the retained lower order PCs, leaving a proportion of the variance unaccounted for. As a rule of thumb, it is generally valid to have twice the number of specimens in each classification group as there are shape variables and computationally stable results will require many more cases than variables.³⁶

In this study we have used PCA to reduce the dimensionality of the shape data and then applied a tuning parameter (p) to limit the number of principal components used in order to optimise the classification, whilst still retaining as large a number of shape variables as possible.

The analysis was undertaken using the *shapes* library³⁰ on the first p PC scores derived from Procrustes analysis, with reliability of classification based on leave-one-out cross-validation with permutation test for significance. The use of a tuning parameter (rather than the commonly used stepwise entry of independent variables) is to limit the effects of over-fitting of data to the discriminant function which can lead to poor out of sample predictive performance. With high dimensional data it is easily possible to get 100% classification within the training sample on the basis of high-order 'noisy' PCs alone, but very poor out of sample classification; lower order PCs are therefore used as these will not be so affected by the specific noise in the sample. Classification by sex was obtained from the discriminant analysis with $p=10$ (thus using PC1

to PC10) with lower classification rates for higher order PCs which were therefore rejected from the analysis.

Using $k=53$ landmarks (of which $p=10$ PCs are retained in the classification) the resulting shape variables successfully classified 85.0% of individuals by biological sex (Table 3). Procrustes ANOVA of shape residuals indicates a statistically significant shape difference between the male and female mean shapes ($F=24.33$, $p<0.0001$).

Table 3. Cross-classification results of sex assessment based on $k=53$ landmarks and $p=9$ PC's (overall cross-validated success rate 85.0%).

	Predicted as male	Predicted as female	Total
Known male	88.0%	12.0%	100%
Known female	18.0%	82.0%	100%

For the final part of the analysis we investigated the impact of landmark number and location on classification accuracy. The first classification utilised $k=53$ landmarks from which $p=10$ shape variables are retained in the classification. We used a two-block partial least squares analysis (PLS) in order to investigate whether classification accuracy can be improved by utilising either a smaller more constrained anatomical region from the OPG or fewer landmarks overall. PLS examines co-variation between two or more sets of variables and identifies features of shape that most strongly co-vary between blocks; this technique is increasingly being used for studying patterns of integration of parts within single configurations of landmarks thus allowing for an assessment of anatomical or structural modularity.³⁶⁻⁴² In the present study we use an assessment of modularity to investigate whether anatomical regions (specifically the mandibular corpus and ascending ramus) provide better assessment of biological sex if treated as isolated structural units - as seen in previous studies^{7,9,11,21,22} - or if they improve sex assessment when combined into a single anatomical module.

To this end we conducted a two-block PLS within the same configuration using *MorphoJ*.³²

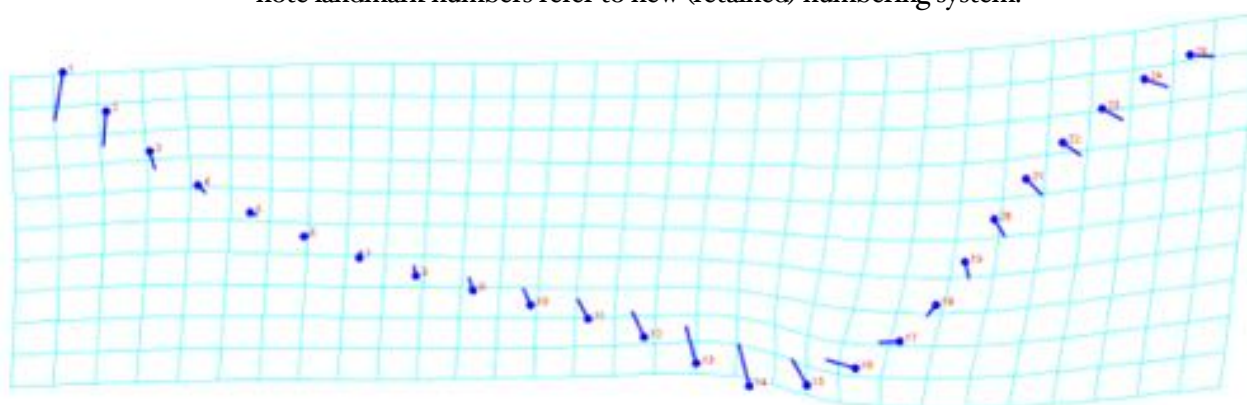
Landmarks were sub-divided into a corpus block ($k_{31} = LM_{1}$ and LM_{4} to LM_{33}) and a ramus block ($k_{22} = LM_{2}$, LM_{3} and LM_{34} to LM_{53}). Two-block PLS produced an *RV* coefficient (the measure of co-variance between units) of 0.74, which indicates a strong statistical association between blocks and a high degree of modularity in anatomical structure; an *RV* of 1 implies that one set of variables can be obtained from the other set by rigid rotation and/or reflection.⁴⁰ To confirm modularity we performed a series of stepwise exclusion tests, reducing 10% of landmarks at each iteration until no improvement in classification accuracy was noted.

Table 4. Cross-classification results of sex assessment based on k_{25} landmarks and $p = 10$ PC's (overall cross-validated success rate 92.5%).

	Predicted as male	Predicted as female	Total
Known male	91.0%	9.0%	100%
Known female	6.0%	94.0%	100%

Re-analysed data was based on treatments of dependent (both blocks) and independent units (single blocks); each iteration required a Procrustes refit with PCA in each round of the stepwise procedure. This reached an optimum classification based on k_{25} landmarks of the dependent blocks (both block sets) with an increased cross-validation of 92.5% of cases by sex (Table 4). Classification rates based on individual treatment blocks were significantly reduced in comparison to the optimal value of k . Optimal sex-based shape differences are significant (Procrustes ANOVA, $F_{24,33}$, $p < 0.0001$) and visualised in Fig. 4; it should be noted that original fixed landmarks LM_{1} to LM_{3} were not retained in the optimal configuration, instead the outline of the inferior corpus and posterior ramus is highlighted by k_{25} retained equidistant landmarks. It can be clearly seen that sex-based differences are localised and most extreme in the inferior displacement of symphysis (LM_{1} to LM_{3} – pointing of the chin), the degree of incurvature in the corpus just anterior to gonion (LM_{8} to LM_{16}) and posterior displacement in the upper half of the posterior border of the ramus (LM_{19} to LM_{25}) in the female mean shape compared to the male.

Fig. 4 Visualization of shape variation due to maximally-differentiating sexual dimorphism as determined by Fisher's linear discriminant analysis based on optimum k_{25} landmarks, showing the extremes of shape variation as vectors. Note, variation is expressed from the male consensus (solid circles) to the female mean shape (terminus of vector), with the deformation grid applied to assist visualization. Figure generated using *MophoJ*; note landmark numbers refer to new (retained) numbering system.



DISCUSSION

This investigation was designed to introduce a more standardised method of sex determination in the process of human identification within the field of forensic dental radiology. The efficacy of cross-validated discriminant analyses indicates a very high level of robust and significant classification based on k_{25} landmarks (92.5% correct overall, 91.0% of males

correctly classified, 94.0% of females correctly classified). These results compare extremely well to earlier research (Table 5) using various methods of metric and statistical shape analysis applied to areas of the mandible such as the gonial region,^{7,22} ascending ramus,^{7,11,21,23} and overall size and shape.^{13,14,16,17,19}

Table 5. Comparison of classification success from the present study compared to other published research. *N* indicates dimensions (2D or 3D) and *K* the number of landmarks utilised (if applicable).

Publication	Classification type	Classification success	N	k
Balci <i>et al.</i> , 2005 ¹¹	Sex assessment based on morphological scoring of traits of ramus flexure using the method of Loth and Henneberg (1996).	Male: 95.6% Female: 70.6% Overall: 90.6%	NA	NA
Franklin <i>et al.</i> , 2007 ¹⁹	Sex assessment from the subadult mandible based on GMM analysis of overall shape	Male: 55% Female: 65% Overall: 59%	3	21
Franklin <i>et al.</i> , 2007 ¹⁶	Sex assessment from adult mandible based on GMM analysis of overall shape	Black male: 85.0% Black female: 90.0% Black overall: 87.5% White male: 88.2% White female: 92.3% White overall: 86.7%	3	38
Franklin <i>et al.</i> , 2008 ¹⁷	Sex assessment from adult mandible based on linear discriminant functions derived inter-landmark distances from 3D shape capture	<i>All variables:</i> Male: 83.3% Female: 84.8% Overall: 84.0% <i>Ramus only:</i> Male: 69.2% Female: 81.9% Overall: 75.1%	3	NA
Kemkes-Grottenthaler <i>et al.</i> , 2002 ⁷	Sex assessment based on morphological scoring of traits of ramus flexure and gonial eversion using the method of Loth and Henneberg (1996).	<i>Ramus flexure:</i> Male: 66% Female: 32% Overall: 59%. <i>Gonial eversion:</i> Males: 75.4% Females: 45.2% Overall: 69.3%	NA	NA
Oettlé <i>et al.</i> , 2005 ²¹	Sex assessment from adult mandible based on GMM analysis of ramus flexure	Male: 67.8% Female: 69.9% Overall: 68.9%	2	11
Oettlé <i>et al.</i> , 2009 ²²	Sex assessment from adult mandible based on GMM analysis of gonial eversion	Male: 73.9% Female: 71.4% Overall: 72.7%	2	7
Pretorius <i>et al.</i> , 2006 ²³	Sex assessment from adult mandible based on GMM analysis of ramus flexure (component of integrated study)	Male: 67.8% Female: 69.9% Overall: 68.9%	2	11
Schmittbuhl <i>et al.</i> , 2001 ¹³	Sex assessment from adult mandible based on elliptical Fourier analysis (size effects included in the analysis)	Male: 97.1% Female: 91.7% Overall: 94.4%	2	NA
Schmittbuhl <i>et al.</i> , 2002 ¹⁴	Sex assessment from adult mandible based on elliptical Fourier analysis (size effects normalised in the analysis)	Male: 84.1% Female: 81.2% Overall: 82.7%	2	NA
Present study	Sex assessment of adult mandible based on GMM analysis of outline of inferior corpus and posterior ascending ramus	Male: 91.0% Female: 94.0% Overall: 92.5%	2	25

Orthopantomogram images allow the objective and reproducible collection of 2D images for the analysis of human variation using geometric morphometric techniques. OPG-derived data was chosen for this analysis because it is both abundant (through clinical treatment) and standardised; many orders of magnitude more data of known age, sex and population group is available from clinical OPG sources than is available from dry bone specimens – as such this is a source of biological data which may be of great future utility for research purposes.

This study confirms that (based on OPG imaging) the dentate mandible exhibits significant sexual dimorphism and that skull assessment of unidentified cadavers cannot leave aside the odontological investigation with the benefit of stored radiological images.

Nevertheless, further assessment on a wider sample of OPGs should be carried out in order to increase the predictive accuracy of this novel methodology. This analysis has demonstrated that the use of OPGs provides a robust standardised method of sex assessment and the importance of performing a complete dental radiological assessment during an autopsy with the aim of human identification of unidentified human remains.⁴³ Stepwise permutation tests and analyses of regional co-variation indicate functional integration in the structure of the mandible, with a high degree of anatomical modularity between the corpus and ramus suggesting that functional ties between the units may co-vary in influencing sex-based

morphological expression. Consequently such units should be studied together (an approach only irregularly applied to date, such as in the application of elliptical Fourier transforms [12-14]) and this may allow for the development of identification criteria based on modular unit shape variables which may be applicable for both whole specimens and fragmented remains depending on the forensic situation.

The success of this proof-of-concept study has encouraged us to expand the remit of the research project, and we will be conducting assessment on a larger sample of OPGs in order to increase the predictive accuracy of sexing and to investigate population-level shape differences. We will expand the biological focus of the analysis and investigate within group (sex and population) as well as pooled sample variation. Furthermore, we will investigate methods of translation of shape variables onto dry bone specimens to aid in sex assessment from skeletonised remains.

CONCLUSION

This preliminary morphometric study confirms that mandible exhibits great sex dimorphism and that radiological OPGs images can be used in the forensic human identification process for sex assessment analysing the geometric and allometry relationship between the corpus and the ascending ramus of the mandible. Further assessment on a wider sample of OPGs should be carried out in order to increase the predictive accuracy of this novel methodology.

REFERENCES

1. Randolph-Quinney P, Mallett X, Black SM. Forensic anthropology. In: Jamieson A, Moenssens A (ed) *Wiley Encyclopedia of Forensic Science*, John Wiley and Son Ltd, London; 2009. pp 152-78.
2. Capitaneanu C, Willems G, Thevissen P. A systematic review of odontological sex estimation methods. *J Forensic Odontostomatol.* 2017 Dec 1;2(35):1-19. Available from: http://www.iofos.eu/Journals/JFOS%20Dec17/JFOS%202-2017_1.pdf [Cited 1 November 2018].
3. Mays S, Cox M. Sex determination in skeletal remains. In: Cox M, Mays S (ed) *Human Osteology in Archaeology*, Greenwich Medical Media Ltd, London; 2000. pp 117-30.
4. St. Hoyme LE, Iscan MY. Determination of sex and race: accuracy and assumptions. In: Iscan MY, Kennedy KAR (ed) *Reconstruction of Life from the Skeleton*, Alan R. Liss Inc, New York; 1989. pp 53-93.
5. Walker PL (2008) Sexing skulls using discriminant function analysis of visually assessed traits. *Am J Phys Anthropol* May; 136 (1):39-50.
6. Wilkinson C. *Forensic Facial Reconstruction*. Cambridge University Press, Cambridge; 2004. pp 456-458.
7. Kemkes-Grottenthaler A, Lobig E, Stock F. Mandibular ramus flexure and gonial eversion as morphologic indicators of sex. *Homo* 2002; 53(2):97-111.
8. Loth SR, Henneberg M. Gonial eversion: facial architecture, not sex. *Homo* Jun 2000; 51(1):81-9.
9. Angel JL, Kelley JO. Inversion of the posterior edge of the jaw ramus: new race trait. In: Gill GW, Rhine S (ed) *Skeletal Attribution of Race: Methods for Forensic Anthropology*. Albuquerque: Maxwell Museum of Anthropology; 1990. pp 33-40.

10. Loth SR, Henneberg M. Mandibular ramus flexure: a new morphologic indicator of sexual dimorphism in the human skeleton. *Am J Phys Anthropol* Mar 1996; 99:473-86.
11. Balci Y, Yavuz MF, Cagdir S. Predictive accuracy of sexing the mandible by ramus flexure. *Homo* 2005; 55(3): 229-37.
12. Badran DH, Othman DA, Thnaibat HW, Amin WM. Predictive accuracy of mandibular ramus flexure as a morphologic indicator of sex dimorphism in Jordanians. *Int J Morphol*. 2015;33(4):1248-54.
13. Schmittbuhl M, Le Minor JM, Taroni E, Mangin P. Sexual dimorphism of the human mandible: demonstration by elliptical Fourier analysis. *Int J Legal Med* Oct 2001;115(2):100-1.
14. Schmittbuhl M, Le Minor J-M, Schaaf A, Mangin P. The human mandible in lateral view: elliptical Fourier descriptors of the outline and their morphological analysis. *Ann Anat* Mar 2002; 184:199-207.
15. Schmittbuhl M, Rieger J, Le Minor JM, Schaaf A, Guy F. Variations of the mandibular shape in extant hominoids: Generic, specific, and subspecific quantification using elliptical Fourier analysis in lateral view. *Am J Phys Anthropol* Jan 2007;132(1):119-31.
16. Franklin D, O'Higgins P, Oxnard C, Dadour I. Sexual dimorphism and population variation in the adult mandible. *Forensic Sci Med Pathol* 2007; 3(1):15-22
17. Franklin D, O'Higgins P, Oxnard CE, Dadour I. Discriminant function sexing of the mandible of indigenous South Africans. *Forensic Sci Int* Jul 2008; 18;179(1):84 e1-5.
18. Buck TJ, Vidarsdottir US. A proposed method for the identification of race in sub-adult skeletons: a geometric morphometric analysis of mandibular morphology. *J Forensic Sci* Nov 2004; 49(6):1-6.
19. Franklin D, Oxnard CE, O'Higgins P, Dadour I. Sexual dimorphism in the subadult mandible: quantification using geometric morphometrics. *J Forensic Sci* Jan 2007; 52(1):6-10.
20. Gonzalez PN, Bernal V, Perez SI. Analysis of sexual dimorphism of craniofacial traits using geometric morphometric techniques. *Int J Osteoarchaeol* 2011; 21(1): 82-91.
21. Oetl  AC, Pretorius E, Steyn M. Geometric morphometric analysis of mandibular ramus flexure. *Am J Phys Anthropol* 2005; 128(3):623-9.
22. Oetl  AC, Pretorius E, Steyn M. Geometric morphometric analysis of the use of mandibular gonial eversion in sex determination. *Homo* 2009; 60(1):29-43.
23. Pretorius E, Steyn M, Scholtz Y. Investigation into the usability of geometric morphometric analysis in assessment of sexual dimorphism. *Am J Phys Anthropol* 2006; 129:64-70.
24. Mitteroecker P, Gunz P. Advances in Geometric Morphometrics. *Evolutionary Biology* 2009; 36:235-47
25. Bookstein FL. *The Measurement of Biological Shape and Shape Change*. Springer Verlag, New York; 1978. pp 159-179.
26. Bookstein FL. *Morphometric Tools for Landmark Data: Geometry and Biology*. Cambridge University Press, Cambridge; 1991. pp 59-66
27. Marcus LF, Corti M, Loy A, Naylor GJP, Slice DE. *Advances in Morphometrics*. Plenum Press, New York; 1996. pp 23-49.
28. Zelditch ML, Swiderski DL, David Sheets H, Fink WL. *Geometric Morphometrics for Biologists*. Elsevier, Oxford; 2004.
29. Zollikofer CPE, Ponce de Leon MS. *Virtual Reconstruction: A Primer in Computer-Assisted Paleontology and Biomedicine*. John Wiley and Sons Inc, Hoboken, New Jersey; 2005.
30. Dryden IL. *Shapes Package*. Vienna, Austria: R Foundation for Statistical Computing; 2012. Available from: <http://www.r-project.org> [Cited 8 August 2018].
31. Claude J. *Morphometrics with R*. Springer, New York; 2008.
32. Klingenberg CP. MorphoJ: an integrated software package for geometric morphometrics. *Molecular Ecology Resources* 2012; 11:353-357.
33. IBM. IBM SPSS Statistics version 20.0; 2012. Available from: <http://www-01.ibm.com/software/analytics/spss> [Cited 8 August 2018].
34. Dryden IL, Mardia KV. *Statistical Shape Analysis*. John Wiley & Sons, Chichester; 1998.
35. Klingenberg CP, Barluenga M, Meyer A. Shape analysis of symmetric structures: quantifying variation among individuals and asymmetry. *Evolution* 2012; 56:1909-20.
36. Mitteroecker P, Bookstein F. Linear discrimination, ordination, and the visualization of selection gradients in modern morphometrics. *Evolutionary Biology* 2011; 38:100-14.
37. Cardini A, Elton S. Sample size and sampling error in geometric morphometric studies of size and shape. *Zoomorphology* 2007; 126:121-34.
38. Bookstein FL, Gunz P, Mitteroecker P, Prossinger H, Schaefer K, Seidler H. Cranial integration in Homo: Singular warps analysis of the midsagittal plane in ontogeny and evolution. *Journal of Human Evolution* 2003; 44:167-87.
39. Bastir M, Rosas A. Hierarchical nature of morphological integration and modularity in the human posterior face. *Am J Phys Anthropol* Sep 2005;128(1): 26-34.
40. Klingenberg CP. Morphometric integration and modularity in configurations of landmarks: tools for evaluating a priori hypotheses. *Evol Dev* 2009; 11:405-21.
41. Mitteroecker P, Bookstein FL. The conceptual and statistical relationship between modularity and morphological integration. *Syst Biol* 2007; 56:818-36.
42. Mitteroecker P, Bookstein FL. The evolutionary role of modularity and integration in the hominid cranium. *Evolution* 2008; 62:943-58.
43. Nuzzolese E, Di Vella G. Digital radiological research in forensic dental investigation: case studies. *Minerva Stomatol* Apr 2012; 61(4):165-73.